Superlattices and Microstructures 122 (2018) 570–576

Contents lists available at ScienceDirect

Superlattices and Microstructures

journal homepage: www.elsevier.com/locate/superlattices

First principles study on the electronic properties and Schottky barrier of Graphene/InSe heterostructure

Khang D. Pham[a,b], Nguyen N. Hieu[c], Victor V. Ilyasov[d], Huynh V. Phuc[e], Bui D. Hoi[f], E. Feddi[g], Nguyen V. Thuan[h], Chuong V. Nguyen[h,*]

[a] Theoretical Physics Research Group, Advanced Institute of Materials Science, Ton Duc Thang University, Ho Chi Minh City, Viet Nam
[b] Faculty of Applied Sciences, Ton Duc Thang University, Ho Chi Minh City, Viet Nam
[c] Institute of Research and Development, Duy Tan University, Da Nang 550000, Viet Nam
[d] Department of Physics, Don State Technical University, Rostov on Don 344000, Russia
[e] Division of Theoretical Physics, Dong Thap University, Dong Thap 870000, Viet Nam
[f] Physics Department, University of Education, Hue University, Hue 530000, Viet Nam
[g] LaMCScI, Group of Optoelectronic of Semiconductors and Nanomaterials, ENSET, Rabat, Mohammed V University in Rabat, Rabat, Morocco
[h] Department of Materials Science and Engineering, Le Quy Don Technical University, Ha Noi 100000, Viet Nam

ARTICLE INFO

Keywords:
Graphene
Indium selenide
Electronic properties
Schottky contact
Strain

ABSTRACT

Graphene-based van der Waals heterostructures by stacking graphene on other two-dimensional materials have recently attracted much attention due to their extraordinary properties and greatly extend the applications of the parent materials. By means of the density functional theory from first-principles calculations, in this work, the electronic properties and Schottky contact of the Graphene/InSe heterostructure, together with the effect of strain, are investigated systematically. Our results show that in the graphene/InSe heterostructure, graphene is very weakly bound to the InSe monolayer. Furthermore, we find that due to the sublattice symmetry breaking, a tiny band gap of 5 meV is opened in the graphene/InSe heterostructure, making it suitable for applications in electronic and optoelectronic devices. Moreover, we also find that the *n*-type Schottky contact is formed in the graphene/InSe heterostructure with a very small Schottky barrier height of 0.05 eV. The Schottky barrier height as well as Schottky contact types in the graphene/InSe heterostructure could be controlled by vertical strain applied perpendicularly to the heterostructure. When the interlayer distance between graphene and the topmost InSe monolayer is smaller than 2.40 Å, one can observe a transformation of the Schottky contact of the graphene/InSe heterostructure. Our results may provide helpful information for designing novel high-performance graphene-based van der Waals heterostructures and explore their potential applications in future nanoelectronic and optoelectronic devices.

1. Introduction

Since its discovery in 2004, graphene (G) has gained remarkable attraction for scientific community owing to its extraordinary atomic, electronic, optical and transport properties, opening up the possibilities for designing novel generation of high-performance nanoelectronic and optoelectronic devices [1–4]. However, the lack of a finite band gap makes G unsuitable for designing logic circuits in electronic devices such as field-effect transistors (FETs) [5]. Thus, in order to use G for application in electronic devices, it

* Corresponding author. Department of Materials Science and Engineering, Le Quy Don Technical University, Ha Noi, Viet Nam.
E-mail addresses: phamdinhkhang@tdt.edu.vn (K.D. Pham), chuongv.nguyen@lqdtu.edu.vn (C.V. Nguyen).

https://doi.org/10.1016/j.spmi.2018.06.049
Received 29 May 2018; Received in revised form 22 June 2018; Accepted 24 June 2018
Available online 26 June 2018

is necessary to creat its finite band gap. Up to date, there exist many efforts to modify a band gap in G, such as adsorption [6], size effect [7], functionalization [8].

In parallel with those mentioned efforts, scientists are recently seeking G-related two-dimensional (2D) materials, which can be used for designing novel high-performance electronic devices. These materials include hexagonal boron nitride (hBN) [9,10], transition metal dichalcogenides (TMDs) [11–14], phosphorene [15,16]. Very recently, a new type of 2D metal dichalcogenide materials, indium selenides (InSe) has been synthesized experimentally [17], showing its potential applications [18–20]. It is clear that in the bulk form, InSe is a semiconductor with a band gap of 1.26 eV [21]. The band gap of InSe crystal decreases with increasing the number of layers owing to quantum confinement [22,23]. Each unit cell of InSe monolayer consists of four covalently bonded Se-In-In-Se atoms. The electronic, magnetic and transport properties of InSe crystals with various allotropes such as bulk, monolayer, and few-layers, have been widely studied both experimentally and theoretically [20,22–24]. For instance, Feng and his co-workers [19] have demonstrated experimentally FET based on InSe multilayer with a high field effect mobility up to 1000 $cm^2V^{-1}s^{-1}$ at the room temperature. Lei and his co-workers [18] have introduced a thin film photodetector with a high photoresponsivity of 34.7 mA/V and a response time of 448 μs. Besides, Debbichi and co-workers [25] have theoretically shown that the band gap of InSe crystal can be transformed from indirect to direct band gap, making it a suitable material for new technology such as the transistors.

Currently, G-based van der Waals (vdW) heterostructures by stacking the G layer on other 2D materials have received considerable interest owing to their outstanding electronic, optical, and thermodynamic properties, which may not occur in parent components. Many G-based vdW heterostructures have recently been studied both experimentally and theoretically. To date, the electronic properties of the combination between G and other metal chalcogenides III-VI compounds, such as G/GaSe [26–28] has theoretically studied. However, the electronic properties and Schottky contact in G/InSe heterostructure have not yet been studied theoretically. Furthermore, a vertical G/InSe heterostructure has been fabricated successfully by mechanically stacking 2D crystals [24]. The results showed that the photodetector based on G/InSe heterostructure has a high photoresponsivity (up to 10^5 AW^{-1}). Therefore, it is necessary to study in details the physical properties of G/InSe heterostructure to better understand the physical mechanisms in the graphene-based 2D vdW heterostructures. In this paper, by means of the density functional theory, we systematically investigate the electronic properties of G/InSe heterostructure, as well as the effect of the interlayer coupling on its electronic properties and Schottky barrier height. The results show a useful information to design and fabricate nanoelectronic and optoelectronic devices based on the G vdW heterostructures.

2. Computational methodology

In the present work, all of our geometric optimization and electronic properties of the G/InSe heterostructure are performed by using first principles calculation based on density functional theory (DFT), that implemented in the simulated Quantum Espresso package [29]. The generalized gradient approximation (GGA) of Perdew-Burk-Ernzerhof (PBE) scheme was used to describe the exchange and correlation potential. Additionally, the projected augmented wave (PAW) potential [30] was also used to describe the electron–ion potential. For the plane wave expansion, the kinetic cut-off energy of 500 eV is used in this work. In order to obtain the geometric lattice parameters of all considered systems, we use the first Brillouin zone (BZ) sampling with $12 \times 12 \times 1$ Monkhorst–Pack *k*–point grid, and the BZ sampling with $9 \times 9 \times 1$ *k*-point grid to perform all the electronic properties calculations. In the present work, the DFT-D2 method proposed by Grimme (DFT-D2) [31] was adopted for describing correctly the non-bonding interaction, existing in the heterostructure. Notice that a semi-empirical dispersion potential was added to the conventional DFT energy in the DFT-D2 method. To avoid artificial interactions with spurious replica images we used a large vacuum region of 20 Å. All geometric structures are fully relaxed until energy and forces are converging to 10^{-6} eV and 0.001 eV/Å, respectively.

3. Results and discussion

Firstly, we design the atomic structure of combining G/InSe heterostructure by using a (2×2) supercell of the InSe monolayer with 8 In atoms and 8 Se atoms and a (3×3) supercell of G with 36 C atoms. The combining G/InSe heterostructure after full geometric relaxation is illustrated in Fig. 1. Notice that in this work, we have considered various stacking configurations of the G/InSe heterostructure. Our results showed that the stacking configuration considered here of the G/InSe heterostructure is the most energetically favorable configuration owing to its lowest total energy. It is well known that electronic properties of InSe monolayer are very sensitive to other external conditions, such as strain [32], thus to design the G/InSe heterostructure we keep the lattice parameters of InSe monolayer fixed, and stretch the lattice parameters of G layer. The lattice mismatch between InSe layer and G layer in the G/InSe heterostructure is small of about 3%. Such small lattice mismatch has no significant effect on the electronic structure [33,34]. Our calculated equivalent interlayer distance *d* between graphene layer and the topmost InSe layer is 3.34 Å. We find that this distance is in the same order of magnitude as the interlayer distances in other vdW G-based heterostructures, such as G/P [35,36], G/WSe_2 [37], G/MoS_2 [38,39], G/ZnO [40]. Thus, the interaction between G and InSe in the G/InSe heterostructure is a typical vdW interaction. Moreover, in order to determine the stability of the G/InSe heterostructure, we also calculate its binding energy as follows: $E_b = [E_{G/InSe} - E_G - E_{InSe}]/N$, where $E_{G/InSe}$, E_G, and E_{InSe} are the total energy of the G/InSe heterostructure, the freestanding G, and the isolated InSe monolayer, respectively. *N* is the number of carbon atoms in the heterostructure. Our calculated binding energy per carbon atom in the G/InSe heterostructure is -40 meV. It is interesting to note that the value of such binding energy has the same order of magnitude as that in other vdW graphene-based heterostructures, such as G/P [35,36], G/WSe_2 [37], G/MoS_2 [38,39], G/ZnO [40]. From the above mentioned point, one can conclude that in the G/InSe heterostructures, the G is bound to the InSe monolayer by the weak vdW interaction.

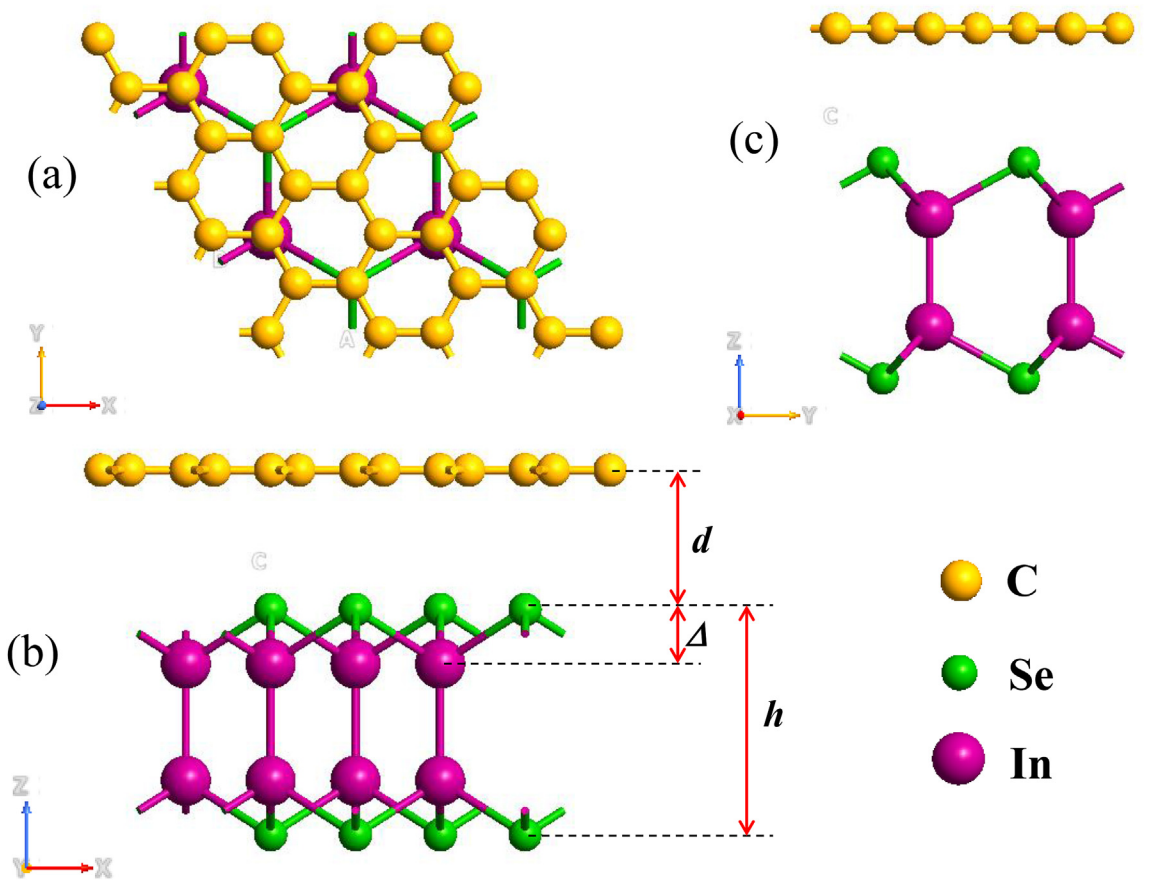

Fig. 1. (a) Top view and (b,c) side views of the relaxed atomic structure of the G/InSe heterostructure.

In addition, in order to study systematically the electronic properties of G/InSe heterostructure, we calculate the band structures of the freestanding G and the isolated InSe monolayer, as shown in Fig. 2(a) and (b), respectively. It can be seen that at the equilibrium state, the freestanding G has a zero band gap with the linear dispersion, which crosses the Fermi level at the high symmetry Dirac *K* point. Unlike graphene, the InSe monolayer is an indirect semiconductor with a band gap of 1.54 eV, forming between the conduction band minimum (CBM) at the Γ point and the valence band maximum (VBM) at the Γ–*K* path, as shown in Fig. 2(b). This result is in good agreement with the previous results [23,32,41,42]. The projected band structure of the combining G/InSe heterostructure is shown in Fig. 2(c). We find that in comparison with the band structures of the freestanding G and the isolated InSe monolayer, the electronic band structure of the G/InSe heterostructure seems to be a sum of those. It means that the electronic properties of the G/InSe heterostructure are well preserved upon contact. The reason is due to the weak vdW interaction, occurring between the G and InSe layers in the G/InSe heterostructure as we have mentioned above. Moreover, we find that in the freestanding form, InSe monolayer is a *p*-type semiconductor, whereas it becomes an *n*-type semiconductor in the G/InSe heterostructure. The nature of this transformation can be explained via the position of Fermi energy level, corresponding to the CBM and VBM of the G/InSe heterostructure. One can observe that the Fermi level in the G/InSe heterostructure shifts upwards from the VBM to the CBM of the InSe semiconductor, resulting in a transformation from the *p*-type to the *n*-type behavior.

In order to provide a more in-depth view of the charge transfer between the G and InSe layers, in Fig. 3 we show the electrostatic potential and the charge density difference of the G/InSe heterostructure at the equilibrium interlayer distance $d = 3.34$ Å along the *z*-direction. One can firstly observe from Fig. 3(a) that the G layer has a deeper electrostatic potential than that of the InSe layer, resulting in a large potential drop across the *z*-direction of the heterostructure. A large potential drop across the *z*-direction of the considered heterostructure here is 26.5 eV. In addition, it should be noted that a large potential drop in the G/InSe heterostructure affects strongly on the carrier dynamics and charge injection and thus may affect on the performance of the graphene-based nanoelectronic devices. When graphene stacked on the InSe monolayer, one can observe that the charge is redistributed in the G/InSe heterostructure. Thus, it is necessary to understand the charge transfer mechanism and the effect of the interface dipole in the G/InSe heterostructure. In Fig. 3(b and c) we present the charge density difference between the G layer and InSe layer in the considered heterostructure. The charge density difference can be visualized as follows: $\Delta\rho = \rho_{G/InSe} - \rho_G - \rho_{InSe}$, where $\rho_{G/InSe}$, ρ_G, and ρ_{InSe}, respectively, are the charge densities of the G/InSe heterostructure, the freestanding G layer, and isolated InSe monolayer. We find that at the equilibrium interlayer distance $d = 3.34$ Å, charge accumulated in the InSe layer, and depleted in the G layer, indicating

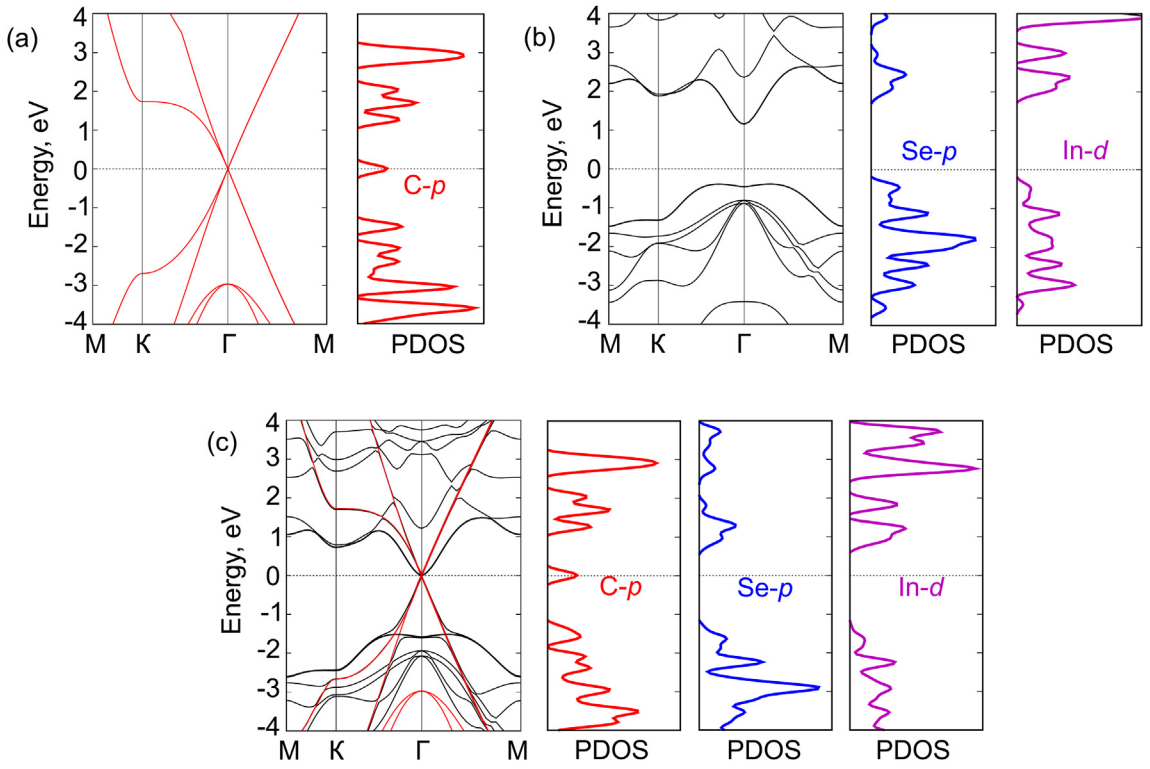

Fig. 2. Calculated band structures and projected density of states in (a) freestanding G, (b) isolated InSe monolayer, and (c) G/InSe heterostructure. The Fermi level is set to be zero. The red and black lines in Fig. 2 (c) correspond to the projected bands of graphene and InSe layer in the G/InSe heterostructure, respectively. (For interpretation of the references to colour in this figure legend, the reader is referred to the Web version of this article.)

that charge transferred from the G layer to the InSe monolayer.

Interestingly, we find that the Schottky contact type can be formed in the G/InSe heterostructure. Based on the Schottky–Mott model, which was presented earlier by Bardeeen [43] for metal/semiconductor heterostructure, an *n*-type Schottky barrier height (SBH) defining by $\Phi_{B,n}$ can be calculated by the energy difference between the Fermi level, E_F, and the CBM, E_{CBM}, that is $\Phi_{B,n} = E_{CBM} - E_F$. Whereas, a *p*-type SBH defining by $\Phi_{B,p}$ is calculated as the energy difference between the E_F and the VBM, that is $\Phi_{B,p} = E_F - E_{VBM}$. For the semiconducting InSe, we find that the sum $\Phi_{B,n}$ and is approximately equal to the E_g. At the equilibrium state, the G/InSe heterostructure forms an *n*-type Schottky contact with a very small SBH of 0.05 eV. The *p*-type SBH of the G/InSe heterostructure is 1.48 eV. Moreover, the work function of graphene is calculated as 4.56 eV, while the electron affinity of the InSe monolayer is calculated to be 4.55 eV. It indicates that the work function of the G is very close to the electron affinity of InSe monolayer, forming an *n*-type Schottky contact. Additionally, a tiny band gap of 5 meV is opened around the Fermi level of the G in the G/InSe heterostructure, making it suitable for application in electronic devices.

We next investigate the effect of the interlayer distance on the electronic properties and the Schottky barrier of the G/InSe heterostructure. It should be noted that the vertical strain applied perpendicularly to the heterostructure, which has widely used to control the electronic properties and Schottky contact of the vdW heterostructures, can be easily achieved by experimental techniques. Thus, the study of the effect of vertical strain on their properties of the G/InSe heterostructure plays an important role for designing novel high-performance Schottky devices in the future. The vertical strain is applied by varying the interlayer distance *d*. In Fig. 4(a) we present the dependence of the SBH on the interlayer distance *d*. We find that the SBH of the G/InSe heterostructure can be controlled by changing the interlayer distance *d*. It can be seen from Fig. 4(a) that with decreasing the interlayer distance *d*, the *n*-type SBH increases, whereas the *p*-type SBH decreases. Moreover, when the interlayer distance *d* is smaller than 2.40 Å, the *n*-type SBH becomes larger than that of the *p*-type, resulting in a transition of the Schottky contact from the *n*-type to the *p*-type. It implies that the vertical strain *d* can control not only the SBH but also the Schottky contact types. Fig. 4(b) we present the electrostatic potential of the G/InSe heterostructure as functions of the interlayer distance *d*. One can observe that with decreasing the interlayer distance *d* more electrons are transferred from the G layer to the InSe layer, resulting in an enhancement of the interlayer interaction between the G layer and InSe layer in the G/InSe heterostructure.

In order to have a deeper insight to the electronic properties of the G/InSe heterostructure under vertical strain, we further consider its band structures under different strains, as shown in Fig. 5. It can be seen that with increasing the interlayer distance *d* from 2.40 Å to 4.28 Å, the Fermi level shifts upwards from the valence band to the conduction band of the semiconducting InSe, resulting in a decrease in the *n*-type SBH of the G/InSe heterostructure from 0.82 eV to 0.01 eV, respectively. Similarly, with

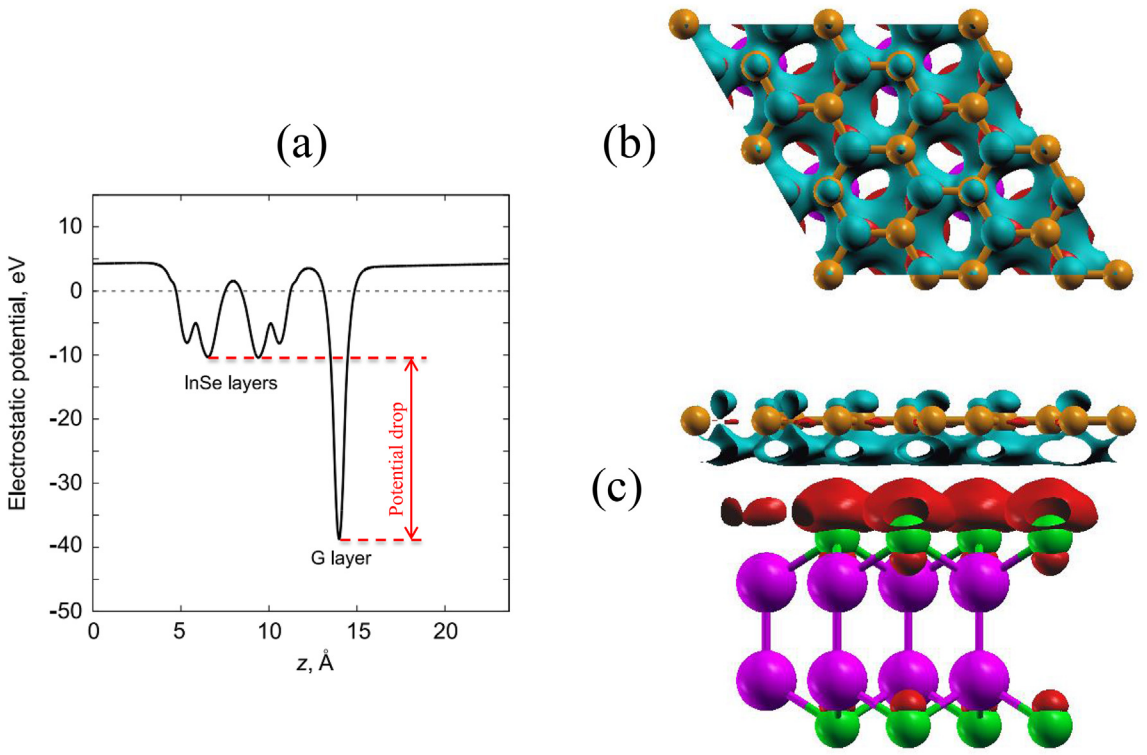

Fig. 3. (a) Electrostatic potential of the G/InSe heterostructure along the *z*-direction and (b) top and side views of the charge density difference of the G/InSe heterostructure along the *z*-direction at the equilibrium state. Red and blue isosurfaces correspond to the accumulation and depletion of electronic densities. The isovalue is set to be 2×10^{-4} $e/Å^3$. (For interpretation of the references to colour in this figure legend, the reader is referred to the Web version of this article.)

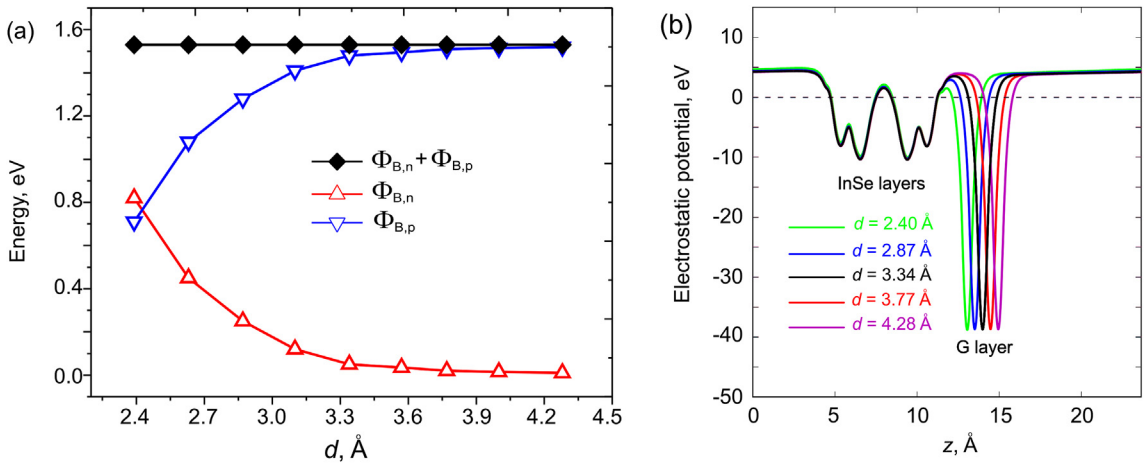

Fig. 4. The dependence of (a) the Schottky barrier height and (b) the electrostatic potential on the interlayer distance of the G/InSe heterostructure.

increasing the interlayer distance, the Fermi level moves upwards from the valence band to the conduction band of the semiconducting InSe, resulting in an increase in the *p*-type SBH of the G/InSe heterostructure. The corresponding *p*-type SBH of the G/InSe heterostructure at the interlayer distance of 2.40 Å, 3.34 Å, and 4.28 Å is 0.71 eV, 1.48 eV, and 1.52 eV, respectively. Additionally, we find that at the interlayer distance $d = 2.40$ Å, the *n*-type SBH becomes larger than that of the *p*-type in the G/InSe heterostructure. It means that a transformation of the Schottky contact in the G/InSe heterostructure from the *n*-type to the *p*-type was observed when the interlayer distance *d* is smaller than 2.40 Å. The nature of this transformation can be understood as follows: when the interlayer distance decreases, the interaction between the G and InSe layers in the G/InSe heterostructure is stronger, resulting in more electrons transfer from the G layer to the InSe layer. With increasing the interlayer distance to 4.28 Å, the *n*-type SBH decreases to 0.01 eV, whereas the *p*-type SBH increases to 1.52 eV. Although the *n*-type SBH of the G/InSe heterostructure decreases to a very

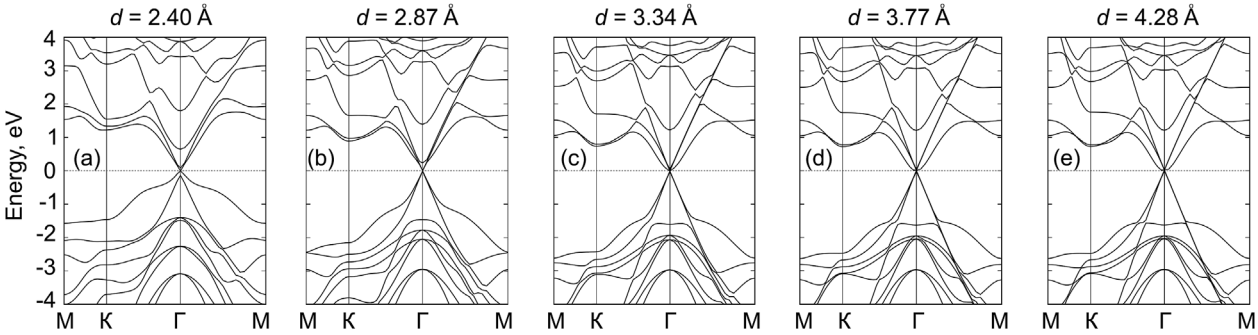

Fig. 5. Band structures of the G/InSe heterostructure under different interlayer distances of (a) 2.40 Å, (b) 2.87 Å, (c) 3.34 Å, (d) 3.77 Å, and (e) 4.28 Å, respectively. The Fermi level is set to be zero.

small of 0.01 eV when the interlayer distance increases to 4.28 Å, however, it is challenging to observe the transition from Schottky contact to the Ohmic contact in the G/InSe heterostructure by applying only vertical strain. Thus, with increasing the interlayer distance *d*, the G/InSe heterostructure keeps an *n*-type Schottky contact, but it is transformed to a *p*-type Schottky contact when the interlayer distance *d* is smaller than 2.40 Å. This transformation of the Schottky contact in the G/InSe heterostructure from the *n*-type to the *p*-type plays an very important role for designing the Schottky devices based on the G/InSe heterostructure.

4. Conclusions

In summary, we have investigated systematically the electronic properties and Schottky contact of the vdW graphene-based heterostructure by combining the graphene and the InSe monolayer using DFT calculations. Our results showed that the interaction between the graphene and the InSe monolayer is the weak vdW interaction, with the interlayer distance between the graphene and the topmost InSe monolayer of 3.34 Å, and the binding energy of −40 meV per carbon atom. Additionally, the G/InSe heterostructure represents a metal/semiconductor heterostructure and forms an *n*-type Schottky contact with a small SBH of 0.05 eV. The effect of vertical strain applied in the G/InSe heterostructure by varying the interlayer distance *d* has also been considered. The results showed that the vertical strain can modulate both the SBH and the Schottky contact types in the G/InSe heterostructure. A transformation from the *n*-type Schottky contact to the *p*-type one was observed in the G/InSe heterostructure when the interlayer distance *d* is smaller than 2.40 Å.

Acknowledgements

This research is funded by Vietnam National Foundation for Science and Technology Development (NAFOSTED) under Grant Number 103.01-2016.07.

References

[1] K.S. Novoselov, A.K. Geim, S.V. Morozov, D. Jiang, Y. Zhang, S.V. Dubonos, I.V. Grigorieva, A.A. Firsov, Science 306 (2004) 666.
[2] K.S. Novoselov, A.K. Geim, S. Morozov, D. Jiang, M. Katsnelson, I. Grigorieva, S. Dubonos, A. Firsov, Nature 438 (2005) 197.
[3] A.C. Neto, F. Guinea, N.M. Peres, K.S. Novoselov, A.K. Geim, Rev. Mod. Phys. 81 (2009) 109.
[4] Q. Tang, Z. Zhou, Prog. Mater. Sci. 58 (2013) 1244.
[5] F. Schwierz, Nat. Nanotechnol. 5 (2010) 487.
[6] R. Balog, B. Jørgensen, L. Nilsson, M. Andersen, E. Rienks, M. Bianchi, M. Fanetti, E. Lægsgaard, A. Baraldi, S. Lizzit, Z. Sljivancanin, F. Besenbacher, B. Hammer, T.G. Pedersen, P. Hofmann, L. Hornekær, Nat. Mater. 9 (2010) 315.
[7] M.Y. Han, B. Özyilmaz, Y. Zhang, P. Kim, Phys. Rev. Lett. 98 (2007) 206805.
[8] Q. Tang, Z. Zhou, Z. Chen, Nanoscale 5 (2013) 4541.
[9] C.R. Dean, A.F. Young, I. Meric, C. Lee, L. Wang, S. Sorgenfrei, K. Watanabe, T. Taniguchi, P. Kim, K.L. Shepard, J. Hone, Nat. Nanotechnol. 5 (2010) 722.
[10] L. Song, L. Ci, H. Lu, P.B. Sorokin, C. Jin, J. Ni, A.G. Kvashnin, D.G. Kvashnin, J. Lou, B.I. Yakobson, P.M. Ajayan, Nano Lett. 10 (2010) 3209.
[11] X. Huang, Z. Zeng, H. Zhang, Chem. Soc. Rev. 42 (2013) 1934.
[12] C.V. Nguyen, N.N. Hieu, N.A. Poklonski, V.V. Ilyasov, L. Dinh, T.C. Phong, L.V. Tung, H.V. Phuc, Phys. Rev. B 96 (2017) 125411.
[13] Q.H. Wang, K. Kalantar-Zadeh, A. Kis, J.N. Coleman, M.S. Strano, Nat. Nanotechnol. 7 (2012) 699.
[14] W.S. Yun, S. Han, S.C. Hong, I.G. Kim, J. Lee, Phys. Rev. B 85 (2012) 033305.
[15] C.V. Nguyen, N.N. Hieu, C.A. Duque, D.Q. Khoa, N.V. Hieu, L.V. Tung, H.V. Phuc, J. Appl. Phys. 121 (2017) 045107.
[16] E.S. Reich, Nature 506 (2014) 19.
[17] W. Huang, L. Gan, H. Li, Y. Ma, T. Zhai, CrystEngComm 18 (2016) 3968.
[18] S. Lei, L. Ge, S. Najmaei, A. George, R. Kappera, J. Lou, M. Chhowalla, H. Yamaguchi, G. Gupta, R. Vajtai, A.D. Mohite, P.M. Ajayan, ACS Nano 8 (2014) 1263.
[19] W. Feng, W. Zheng, W. Cao, P. Hu, Adv. Mater 26 (2014) 6587.
[20] W. Feng, J.-B. Wu, X. Li, W. Zheng, X. Zhou, K. Xiao, W. Cao, B. Yang, J.-C. Idrobo, L. Basile, W. tian, P. Tan, P. Hu, J. Mater. Chem. C 3 (2015) 7022.
[21] J. Camassel, P. Merle, H. Mathieu, A. Chevy, Phys. Rev. B 17 (1978) 4718.
[22] S. Magorrian, V. Zólyomi, V. Fal'ko, Phys. Rev. B 94 (2016) 245431.
[23] C. Sun, H. Xiang, B. Xu, Y. Xia, J. Yin, Z. Liu, Appl. Phys. Express 9 (2016) 035203.
[24] G.W. Mudd, S.A. Svatek, L. Hague, O. Makarovsky, Z.R. Kudrynskyi, C.J. Mellor, P.H. Beton, L. Eaves, K.S. Novoselov, Z.D. Kovalyuk, E.E. Vdovin, A.J. Marsden, N.R. Wilson, A. Patane, Adv. Mater 27 (2015) 3760.

[25] L. Debbichi, O. Eriksson, S. Lebègue, J. Phys. Chem. Lett. 6 (2015) 3098.
[26] H.V. Phuc, V.V. Ilyasov, N.N. Hieu, B. Amin, C.V. Nguyen, J. Alloy. Comp. 750 (2018) 765.
[27] H.V. Phuc, N.N. Hieu, Bui D. Hoi, Chuong V. Nguyen, Phys. Chem. Chem. Phys. (2018), http://pubs.rsc.org/en/content/articlelanding/2014/cp/c8cp02190b#!divAbstract.
[28] C. Si, Z. Lin, J. Zhou, Z. Sun, 2D Mater. 4 (2016) 015027.
[29] P. Giannozzi, S. Baroni, N. Bonini, M. Calandra, R. Car, C. Cavazzoni, D. Ceresoli, G.L. Chiarotti, M. Cococcioni, I. Dabo, A.D. Corso, S. de Gironcoli, S. Fabris, G. Fratesi, R. Gebauer, U. Gerstmann, C. Gougoussis, A. Kokalj, M. Lazzeri, L. Martin-Samos, N. Marzari, F. Mauri, R. Mazzarello, S. Paolini, A. Pasquarello, L. Paulatto, C. Sbraccia, S. Scandolo, G. Sclauzero, A.P. Seitsonen, A. Smogunov, P. Umari, R.M. Wentzcovitch, J. Phys. Condens. Matter 21 (2009) 395502.
[30] P.E. Blöchl, Phys. Rev. B 50 (1994) 17953.
[31] S. Grimme, Wiley Interdiscip. Rev. Comput. Mol. Sci. 1 (2011) 211.
[32] T. Hu, J. Zhou, J. Dong, Phys. Chem. Chem. Phys. 19 (2017) 21722.
[33] H.V. Phuc, V.V. Ilyasov, N.N. Hieu, C.V. Nguyen, Vacuum 149 (2018) 231.
[34] A. Mattausch, O. Pankratov, Phys. Rev. Lett. 99 (2007) 076802.
[35] J. Padilha, A. Fazzio, A.J. da Silva, Phys. Rev. Lett. 114 (2015) 066803.
[36] M. Sun, J.-P. Chou, J. Yu, W. Tang, Phys. Chem. Chem. Phys. 19 (2017) 17324.
[37] M. Sun, J.-P. Chou, J. Yu, W. Tang, J. Mater. Chem. C 5 (2017) 10383.
[38] C.V. Nguyen, Superlattice. Microst. 116 (2018) 79.
[39] Y. Ma, Y. Dai, M. Guo, C. Niu, B. Huang, Nanoscale 3 (2011) 3883.
[40] P. Xu, Q. Tang, Z. Zhou, Nanotechnology 24 (2013) 305401.
[41] G. Mudd, M. Molas, X. Chen, V. Zólyomi, K. Nogajewski, Z.R. Kudrynskyi, Z.D. Kovalyuk, G. Yusa, O. Makarovsky, L. Eaves, M. Potemski, V.I. Fal'ko, A. Patanè, Sci. Rep. 6 (2016) 39619.
[42] X. Li, C. Xia, X. Song, J. Du, W. Xiong, J. Mater. Sci. 52 (2017) 7207.
[43] J. Bardeen, Phys. Rev. 71 (1947) 717.